A Unit Cube-Based Model for Heat Transfer and Fluid Flow in Porous Carbon Foam

Qijun Yu
Department of Mechanical and Materials Engineering,
The University of Western Ontario,
London, ON, N6A 5B8, Canada
e-mail: yu@fatfoam.com

Brian E. Thompson
Foam Application Technologies Inc.,
Mayaguez, Puerto Rico
e-mail: thompson@fatfoam.com

Anthony G. Straatman[1]
Mem. ASME
Department of Mechanical and Materials Engineering,
The University of Western Ontario,
London, ON, N6A 5B8, Canada
e-mail: astraatman@eng.uwo.ca

A unit-cube geometry model is proposed to characterize the internal structure of porous carbon foam. The unit-cube model is based on interconnected sphere-centered cubes, where the interconnected spheres represent the fluid or void phase. The unit-cube model is used to derive all of the geometric parameters required to calculate the heat transfer and flow through the porous foam. An expression for the effective thermal conductivity is derived based on the unit-cube geometry. Validations show that the conductivity model gives excellent predictions of the effective conductivity as a function of porosity. When combined with existing expressions for the pore-level Nusselt number, the proposed model also yields reasonable predictions of the internal convective heat transfer, but estimates could be improved if a Nusselt number expression for a spherical void phase material were available. Estimates of the fluid pressure drop are shown to be well-described using the Darcy-Forchhiemer law, however, further exploration is required to understand how the permeability and Forchhiemer coefficients vary as a function of porosity and pore diameter. [DOI: 10.1115/1.2165203]

Keywords: porous carbon foam, unit-cube geometry, heat transfer in porous media

1 Introduction

There are essentially two types of porous solids: those produced by packing or sintering solid particles or cylinders together and those produced by casting or foaming a material during solidification. In both cases, the final product consists of interspersed regions of solid and fluid (or void). Depending on the final structure, the void regions may be isolated from one another (trapped phase) or continuous as in the case of an interconnected pore structure. Graphitized porous carbon foam fabricated using the ORNL patented process [1] represents a case of near-spherical interconnected pores, as shown in Fig. 1. The figure illustrates the open, interconnected structure of the foam and the near-homogeneous distribution of void size. Porous carbon foam exhibits unique thermo-physical and geometric characteristics [2] that make it suitable for heat transfer applications in microelectronics and power generation. The unique characteristics include:

1. An extremely high bulk thermal conductivity (stagnant effective thermal conductivity) between 40 and 180 W/m K [2,3]. This high effective conductivity results from the extremely high material conductivity of the graphitized carbon material (k=800–1900 W/m K). In contrast, similar porosity aluminum foams have effective conductivities of approximately 2–26 W/m K, which result from material conductivities of 140–237 W/m K (for aluminum alloys). As such, the carbon foam has a much higher capability to conduct or entrain heat into its internal structure so that infiltrated fluid can convect heat away.
2. An open, inter-connected void structure that enables fluid infiltration such that enormous increases in surface area for heat transfer are available (5000 to 50,000 m^2/m^3).
3. A low density (from 0.2 to 0.6 g/cm^3, depending upon porosity), which makes the material suitable for compact and lightweight applications. In contrast, aluminum foam has a density of 0.3–0.8 g/cm^3, depending upon porosity.
4. An increase in exposed surface area and a rough open structure, which leads to increased mixing at the external fluid interface.

To consider the carbon foam material for heat transfer applications, there is an immediate need for an engineering model that can be used to evaluate the thermal and hydrodynamic characteristics under different operating conditions. For a generic convective heat transfer application, the model is required to express the internal exposed surface area, the external exposed surface area, and the void window size as a function of foam porosity and pore diameter. The model can then be used to produce expressions for the surface roughness, the effective conductivity, and the permeability. The review given below provides a brief overview of previous modeling efforts in porous media and makes clear the need for a new model to characterize porous carbon foam. The review includes efforts to model the geometry, the effective conductivity, and the permeability.

The geometric condition of a porous media is typically characterized by an idealized geometry model from which the internal surface area to volume ratio, β, and all other internal and external geometry parameters can be derived. To this end, Dullien [4] considered a regularly packed bed of spheres and derived the classical expression for the surface area to volume ratio: $\beta=6(1-\varepsilon)/D_p$, where ε is the porosity of the porous media defined as $\varepsilon=V_f/V_{\text{tot}}$, D_p is the particle (sphere) diameter, and the subscript f denotes the fluid or void phase. For the same condition, Hwang et al. [5] used the empirical expression $\beta=20.346(1-\varepsilon)\varepsilon^3/D_p$ to derive an expression for the heat transfer in his experiments on packed spherical particles. The empirical expression is slightly different as it accounts for non-regular packing of the spherical bed whereas the analytical model considers perfectly regular packing. By comparing these expressions, it is evident that β is the same when $\varepsilon=0.67$; for $\varepsilon>0.67$, the empirical expression predicts slightly higher β due to the non-regular void structure. For reticulated metal foams, such as aluminum foam, simplified geometry models take the form of a unit-cell with square-barred corner elements [6]. The size of the square bars is determined

[1]Author to whom correspondence should be sent.

Contributed by the Heat Transfer Division of ASME for publication in the JOURNAL OF HEAT TRANSFER. Manuscript received October 18, 2004; final manuscript received October 24, 2005. Review conducted by Yogesh Jaluria.

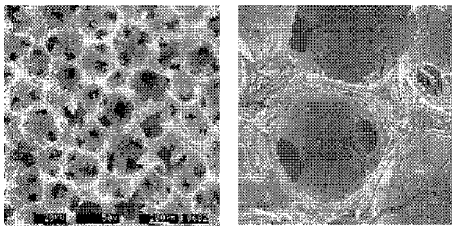

(a) (b)

Fig. 1 (*a*) Electron micrograph of the carbon foam surface [1]; (*b*) electron micrograph of the carbon foam surface of a single pore

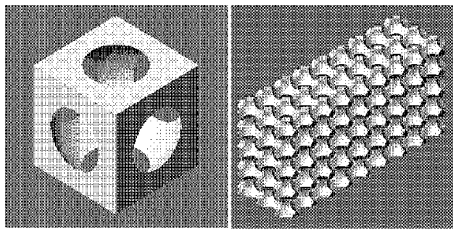

(a) (b)

Fig. 2 CAD images showing the proposed unit-cube model: (*a*) a single unit-cube with spherical void; (*b*) pore block containing a number of interconnected pores

such that the porosity V_f/V_{tot} is preserved. There are no available geometry models for spherical void structures, such as that observed in porous carbon foam. Though this is essentially opposite to the packed-sphere geometry, expressions for internal and external surface areas are different and must be obtained from a new basic geometry model that represents the spherical void phase.

The effective thermal conductivity, k_e, of a porous media can be obtained experimentally by testing several different samples of a specific porous material, or analytically by solving a heat transfer problem for an idealized geometry model. Deissler et al. [7] investigated the effective thermal conductivity of two simple models: two planar layers (i.e., solid and fluid) in parallel and two layers in series. The expression for two layers in parallel is: $k_e = k_f\varepsilon + (1-\varepsilon)k_s$, whereas the expression for two layers in series is: $k_e = k_s/(\varepsilon\sigma + (1-\varepsilon))$, where σ is the ratio of solid phase to void phase conductivities. The two expressions predict effective conductivities with variations as high as 7% for $\sigma=2$, and as high as 99% for $\sigma=1000$ (with $\varepsilon=0.4$). This is due to the fact that when σ is high the solid material arrangement has a great influence on the effective conductivity. As such, for high σ applications such as porous carbon foam, an accurate characterization of the internal geometry is necessary. Batchelor and O'Brien [8] derived an analytical solution for k_e of a packed bed of spheres by solving an integral equation for the temperature distribution over the sphere surface. A thermal-electrical approach was used by several authors (see, for example, Refs. [6,9]) to derive expressions for the effective conductivity of packed sphere geometries of different materials. Bhattacharya et al. [10] used both analytical and empirical relations for determining the effective thermal conductivity of metal foams. Tee et al. [11] integrated a probability density function over randomly distributed cubical cells to obtain an isotropic estimate of the effective conductivity of porous carbon foam. Klett et al. [12] proposed a conductivity model based upon the ligament conductivity and the mean flow path for a spherical void phase. Comparisons with available data for porous carbon foam showed that that the model produced good predictions, but the model parameters must be calibrated to give good characteristic results. A thermal-electrical analogy will be applied in the present study in combination with the proposed geometry model to obtain an expression for the effective thermal conductivity for a spherical void porous material.

The most widely used expression for the permeability of a porous media is the Ergun equation [13] given as: $K = \varepsilon^3 D_p^2/(150(1-\varepsilon)^2)$, however, Nakayama and Kuwahara [14] reviewed available studies on the permeability of various geometric models and proposed $K = \varepsilon^3 D_p^2/(147(1-\varepsilon)^2)$ as the most suitable generic expression for a packed bed of spheres. In the present study, the same permeability expression will be employed, but using an equivalent particle diameter that is derived from the unit-cube geometry proposed to model porous carbon foam. The model will then be calibrated against existing data for fluid pressure drop across porous carbon.

The present study proposes a unit-cube model to characterize the geometry of porous carbon foam or other open, interconnected porous media with a near-spherical void phase. The geometry model is based on a unit-cube-centered sphere, where the sphere represents the fluid or void phase. The complete geometry model is presented and all geometry parameters required for application in convective heat transfer are presented. The unit-cube model is then used to develop an expression for the effective conductivity of the porous material. The model is validated by comparing predictions of the effective conductivity, the internal convective heat transfer and the fluid pressure drop to other modeled results and to previous results obtained experimentally.

2 Geometric Model for Porous Carbon Foam

A geometric model is required for the exploration of heat transfer and flow in terms of the geometry parameters, thereby enabling optimization of the foam structure for different applications. Based on the geometry characteristics of the carbon foam [1–3], the following assumptions for the present geometric model are proposed:

1. The entire foam is assumed to have a single uniform void (pore) diameter.
2. Pores are considered to be spherical and centered inside unit-cubes.
3. Pores are regularly arranged in space, and each pore connects with six adjacent pores on the six surfaces of the unit cube.

Figure 2(*a*) shows a three-dimensional CAD image of the proposed unit-cube geometry with a spherical void phase. Figure 2(*b*) shows a pore block of unit-cubes with exposed pore surfaces that are cut at the center plane of the cube at the sides, front and top of the pore block. Figure 3 compares the internal geometry of the idealized geometry model with similar images of the porous carbon foam obtained from ORNL. The images illustrate that the idealized geometry model effectively captures the internal structure of the carbon foam. Figure 4 shows the detailed dimensions of the unit-cube model. Here, D is the pore (void phase) diameter; $H = f(D,\varepsilon)$ is the height of the unit-cube defined by the given pore diameter and the porosity; $h = (D-H)/2$ is the spherical cap height of the pore; $d = \sqrt{D^2 - H^2}$ is the interconnected pore channel diameter, which is the opening diameter of the pore interface at the unit-cube surface (also called the pore window); and $c = (H-d)/2$ is the width of the strut at the center plane of the unit cube (also called the ligament width).

The size of a unit-cube is not universally constant, rather it is determined by considering the desired porosity and pore diameter. By the definition of porosity [15], an expression relating the cube height H, the porosity ε, and the pore diameter D is derived

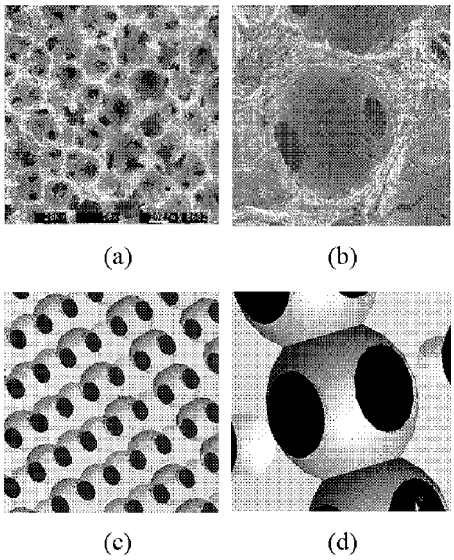

Fig. 3 A comparison of the idealized geometry (*a*) and (*b*) with the structure of porous carbon foam (*c*) and (*d*) obtained from ORNL [1]

$$H^3 - \frac{3\pi D^2}{(4\varepsilon + \pi)}H + \frac{4\pi D^3}{3(4\varepsilon + \pi)} = 0 \tag{1}$$

The dimension of the unit-cube H is obtained by solving Eq. (1) for given values of ε and D. Once the size of the unit-cube is established, the geometry is fixed and the remaining geometric parameters can be evaluated as described below. Since the porous carbon foam has an interconnected pore structure, we are only interested in the range of pore window sizes: $0<d<H(0.52<\varepsilon<0.96)$. When $d\leqslant 0$, the unit-spheres are isolated from one another; for $d\geqslant H, c\leqslant 0$ meaning that the ligaments connecting the solid phase are broken.

For a general application where fluid passes both across and through the porous material, information on the geometry is required for the internal structure and for the external interface between the porous material and the fluid. The internal structure is described here in terms of the area to volume ratio. The external geometry is described in terms of the exposed surface area factor and the absolute roughness of the exposed surface. While the external geometry parameters are only required for cases where fluid flows across the exposed surface, they are included here for completeness and reference.

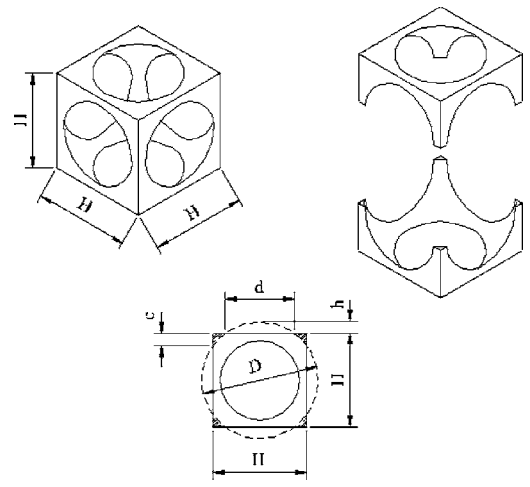

Fig. 4 Detailed dimensions of the unit cube geometry model at a cross section cut at the center plane of the unit cube

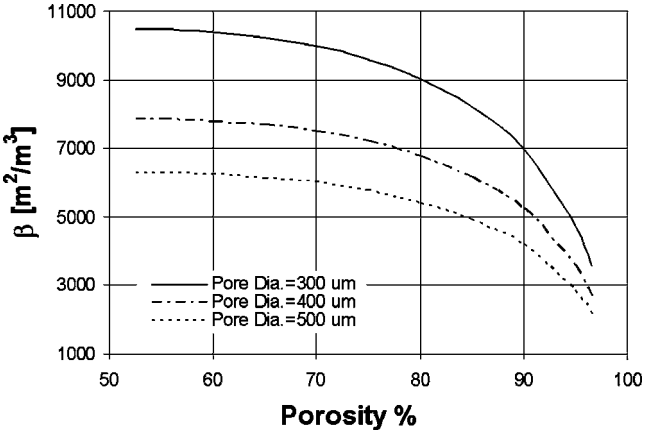

Fig. 5 Interior surface area to volume ratio β plotted as a function of porosity for three different spherical void (pore) diameters

2.1 Interior Surface Area to Volume Ratio β. The ratio β quantifies the internal surface area available for convective heat transfer. For a solid unit-cube, $\beta=0$, which represents the lower limit. For porous carbon foam made by ORNL process [1], this value can be as high as 5000–50,000 m^2/m^3, depending upon the porosity and void diameter. The ratio β of the proposed unit-cube geometry is expressed as: $\beta=S_{\text{int-wall}}/H^3$, where $S_{\text{int-wall}}$ is the void interior surface area in a single unit-cube obtained from:

$$S_{\text{int-wall}} = \pi D^2 - 6(\pi Dh) = \pi D(3H - 2D) \tag{2}$$

giving the final expression

$$\beta = \frac{\pi D}{H^3}(3H - 2D) \tag{3}$$

Figure 5 shows the variation of β for different D over the range $0.52<\varepsilon<0.96$, which corresponds to the limits described following Eq. (1). Here it is evident that β decreases with increasing porosity and with increasing void diameter. For high porosities, β decreases sharply due to the decrease in available solid material inside the foam. For a convective heat transfer application, the optimal value for β is evaluated by comparison of the thermal and hydrodynamic resistances. The higher the value of β, the higher the area available for internal heat exchange but this also results in higher net viscous losses resulting in a higher fluid pressure drop.

2.2 External Exposed Surface Area. To characterize surface area on the external surfaces of the foam, we introduce a surface area factor S_F, defined as the ratio of the total average open pore surface area over the flat surface area of the cube at the exposed layer, that is

$$S_F = \frac{S_{\text{exp}}}{H^2} \tag{4}$$

The exposed surface area, S_{exp}, of the open pore structure represents the interface between the pure fluid domain and the porous domain represented by the idealized geometry model. Since the exposed interface depends upon the location of the cut, the exposed surface area is obtained by considering an average location. The exposed surface includes two parts: (1) the flat cross-section surface area cut at a location either between 0 and c or c and $H/2$; and (2) the opened pore spherical wall surface area (see Fig. 6). The flat cross-section surface area is computed from two portions: from 0 to c and from c to $H/2$. The detailed dimensions used to compute the flat cross-section surface area are shown in Fig. 7.

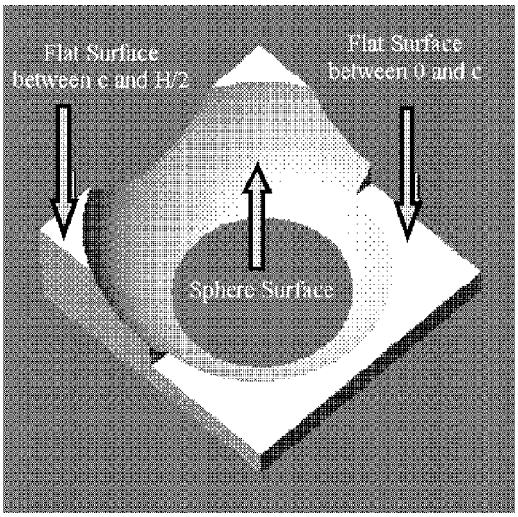

Fig. 6 Illustration of the exposed pore surface area showing the spherical wall surface and the flat surface cross section cut at a location either between 0 and *c* or between *c* and *H*/2

The flat surface area S_{1y} from 0 to c is obtained as

$$S_{1y} = H^2 - \pi r^2 \tag{5}$$

where $r^2 = R^2 - H'^2$, and $H' = H/2 - y$. The average flat cross-section surface area from 0 to c is then calculated to be

$$S_{\text{avg1}} = \frac{1}{c}\int_0^c S_{1y}dy \tag{6}$$

The flat surface area S_{2y} from c to $H/2$ is obtained from

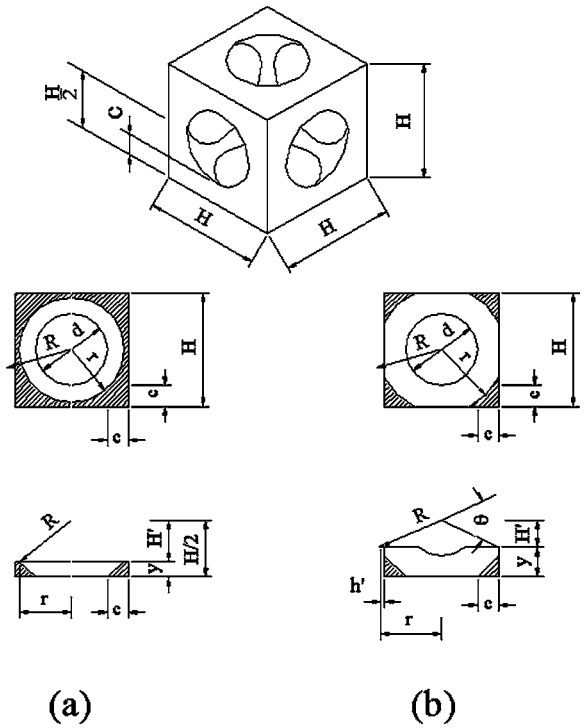

Fig. 7 (*a*) Flat cross-section surface cut at a location between 0 and *c*; (*b*) flat cross-section surface cut at a location between *c* and *H*/2

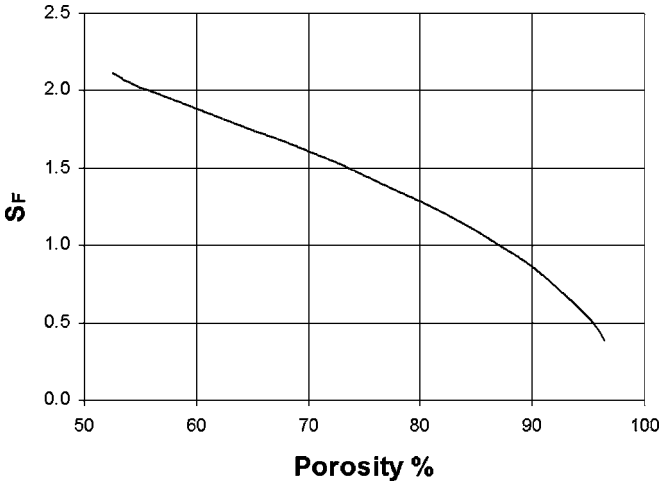

Fig. 8 Plot showing the variation of the surface area factor, S_F, as a function of porosity

$$S_{2y} = H^2 - \left(\pi r^2 - 4\frac{r^2}{2}(\theta - \sin\theta)\right) \tag{7}$$

where r and H' for S_{2y} are the same as that described above for S_{1y}, and $\theta = 2\cos(H/2r)$. The average flat cross-section surface area from c to $H/2$ is determined to be

$$S_{\text{avg2}} = \frac{1}{\left(\frac{H}{2} - c\right)}\int_c^{H/2} S_{2y}dy \tag{8}$$

Then the average flat cross-section area from 0 to $H/2$, S_{favg}, is obtained by averaging S_{1y} and S_{2y} over H, and is expressed by

$$S_{\text{favg}} = \frac{2\left(S_{\text{avg1}}c + S_{\text{avg2}}\left(\frac{H}{2} - c\right)\right)}{H} \tag{9}$$

The opened spherical wall surface area, S_s, is given by (assuming the pore is cut at the pore center plane)

$$S_s = \frac{S_{\text{int-wall}}}{2} \tag{10}$$

Finally, the total average opened surface area at the exposed layer, S_{exp}, is the sum of S_{favg} and S_s, and is given by

$$S_{\text{exp}} = S_{\text{favg}} + S_s \tag{11}$$

which is inserted into Eq. (4). Figure 8 shows the relationship between the surface area factor S_F and the porosity for a fixed pore diameter. It is found that the exposed surface area factor S_F decreases as the porosity increases and it reaches a maximum value of 2.15 at a porosity of 0.5236, and a value of 1 at porosity of 0.8722. This means that if a fluid flowing across the foam does not penetrate the foam surface, the available area for heat transfer is the same as that of a smooth plate (of the same plan dimensions) when $\varepsilon = 0.8722$. For the more commonly observed case where the fluid penetrates the foam, large increases in surface area are made available, resulting in increased heat transfer.

2.3 Absolute Surface Roughness of the Exposed Pore Surface R_A. The absolute surface roughness of the exposed pore surface is required to determine the resistance due to the open surface for applications where the flow is not forced directly into the foam. R_A is defined as the radius of the inter-connected pore diameter (radius of the pore window) and is determined by

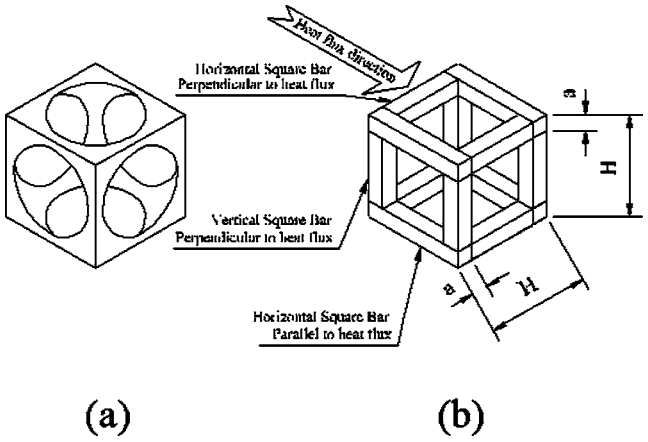

Fig. 9 (*a*) Carbon foam-spherical void phase pore structure; (*b*) equivalent solid square bar structure with the same porosity

$$R_A = \frac{d}{2} = \frac{1}{2}\sqrt{D^2 - H^2} \tag{12}$$

Parameters of the geometric model are now used to develop an analytical model for the effective thermal conductivity of the unit-cube structure and for the hydrodynamic loss associated with flow through the porous material.

3 Thermal Model

The thermal model consists of two parts and is required for the application of the unit-cube model in engineering calculations. The effective thermal conductivity is required to quantify the rate at which energy is entrained into the foam structure and the convective model to quantify the rate at which energy can be removed by the infiltrated fluid.

3.1 Effective Thermal Conductivity. The effective or stagnant thermal conductivity of a porous material is a function of the thermal conductivities of the solid and the fluid, the porosity and the structure of the foam, and is another important parameter characterizing the porous material. The equivalency technique is applied to the solid phase volume since the solid phase is the controlling factor for the effective thermal conductivity of the porous carbon foam material. The effective thermal conductivity is based on the following assumptions:

1. No air flow exists in the inter-connected pore channel. Therefore, no convection between the air and the solid takes place in the pore channel.
2. There is no net radiation heat transfer in the inter-connected pore channel.
3. A local thermal equilibrium exists between the solid and fluid phases at the pore level, which means that the temperature difference between the solid and void phases is negligible.

Figure 9 shows the volume equivalency process for simplifying the pore-level geometry while preserving the volume ratio of solid/fluid (porosity). The square bar size a is determined by solving the following cubic equation obtained from the volume equivalency

$$a^3 - \frac{3}{4}a^2 - \frac{1-\varepsilon}{16}H^3 = 0 \tag{13}$$

Figure 10 shows the details of the equivalency and electrical analogy processes used to obtain the effective thermal conductivity of the carbon foam. The equivalent square bar structure is first divided into parallel and series parts as shown in Fig. 10(*b*). The

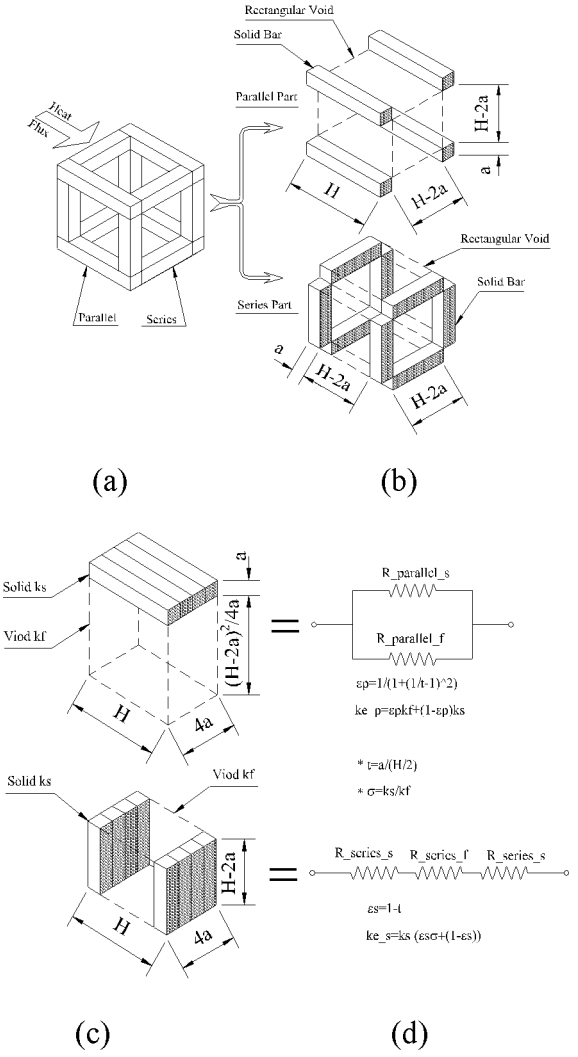

Fig. 10 (*a*) Square bar equivalent for thermal-electric analogy; (*b*) equivalent parallel and series parts; (*c*) simplified parallel and series parts; (*d*) equivalent heat transfer circuits

parallel and series parts are then converted into the simple forms shown in Fig. 10(*c*) by applying the equivalency method to the volume. The top view of Fig. 10(*d*) shows the equivalent heat transfer circuit that represents the parallel part, and the bottom view shows the equivalent heat transfer circuit that represents the series part. The simplified parallel part is presented as a pure parallel circuit consisting of the solid and void parts as shown in the top view of Fig. 10(*d*), and its effective thermal conductivity k_{ep} is calculated by [9]

$$k_{ep} = \frac{\left(\frac{1}{t} - 1\right)^2 + \sigma}{\left(\frac{1}{t} - 1\right)^2 + 1} k_f \tag{14}$$

where k_f is the thermal conductivity of the fluid and k_s for the solid, $t = 2a/H$ is the normalized thickness of the square bar, and σ is the ratio of the thermal conductivity of the solid phase to the fluid phase: $\sigma = k_s/k_f$. The simplified series part is represented as a pure series circuit consisting of the solid and void parts as shown in the bottom view of Fig. 10(*d*), and its effective thermal conductivity k_{es} is calculated as [9]

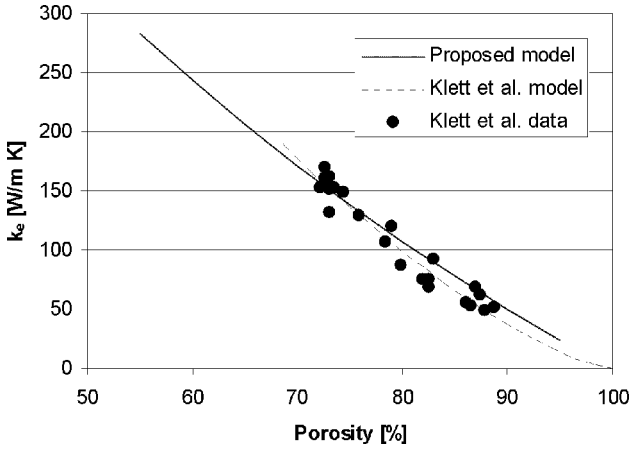

Fig. 11 Plot showing the effective thermal conductivity of porous carbon foam as a function of porosity for k_s =1300 W/m K

$$k_{es} = \frac{k_s}{(1-t)\sigma + t} \tag{15}$$

The effective thermal conductivity of a porous material is given by

$$k_e = \varepsilon_e k_{ep} + (1-\varepsilon_e)k_{es} \tag{16}$$

where ε_e is the volume ratio of the parallel part to the sum of the series part and the parallel part, and is determined by

$$\varepsilon_e = 1 - 2t + 2t^2 \tag{17}$$

When Eqs. (14), (15), and (17) are substituted into Eq. (16), the final expression for the effective thermal conductivity of the spherical void porous material is obtained

$$k_e = (1-2t-2t^2)\left(\frac{\left(\frac{1}{t}-1\right)^2 + \sigma}{\left(\frac{1}{t}-1\right)^2 + 1}\right)k_f + \frac{2t(1-t)}{(1-t)\sigma + t}k_s \tag{18}$$

Figure 11 shows the variation of k_e with ε as predicted by Eq. (18) (solid line). The effective conductivity is seen to decrease with increasing porosity due to the reduction of solid phase material with increasing ε. Included in Fig. 11 is measured data reported by Klett et al. [12]; the data were converted from density to porosity form assuming a ligament density of 2.23 g/cm^3 [12]. Figure 11 also compares predictions of the model relation developed by Klett et al. [12]. It is clear from the figure that both models are in good agreement with the measured data. The virtue of the present model is that there are no parameters to adjust; the predicted result is obtained using the geometry of the foam and the solid and fluid phase thermal conductivities only. As such, the proposed model can be applied in engineering heat transfer models and in computational fluid dynamics codes without special tuning.

It is important to note that the heat transfer is not dictated by the effective conductivity alone. That is, for low porosity, the effective conductivity is high, which means that heat is readily transferred into the porous material, but it is difficult for fluid to penetrate the foam resulting in lower convection and an imbalance in the conductive-convective resistances. For high porosity, the effective conductivity is low meaning that conduction into the foam is low, but it is easy for fluid to penetrate the foam so the convective resistance is lower. As such, the optimal porosity must be obtained by considering the rate at which heat is transferred into the foam and the rate at which heat can be removed by internal convection.

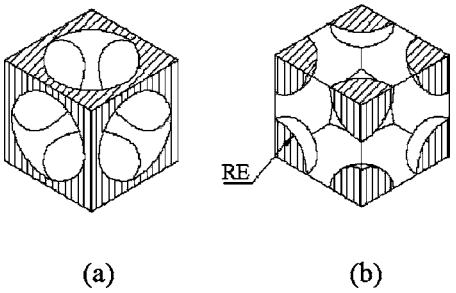

Fig. 12 Graphical representation of the equivalent sphere particle diameter: (*a*) the actual spherical void phase and (*b*) the equivalent solid particle obtained from Eq. (21)

3.2 Convective Heat Transfer. The convective heat transfer can be estimated using the internal area factor β combined with an appropriate relation for the internal, pore-level Nusselt number. Though no known relation exists specifically for a spherical void phase porous material, reasonable estimates of heat transfer can be obtained from relations for porous materials with an interconnected internal structure. To this end, studies have been conducted to quantify the internal convective heat transfer and pressure drop across porous media with an interconnected void structure (Refs. [4,16]). Additional reviews have been compiled by Bear and Corapcioglu [17–19] and Kakac et al. [20]. Recent studies on the fundamentals and applications of the flow and heat transfer in porous media have also been edited in detail by Vafai et al. [21]. Gamson et al. [22] proposed

$$\mathrm{Nu}_{sf} = 1.064\,\mathrm{Re}_d^{0.59}\mathrm{Pr}^{1/3} \tag{19}$$

for turbulent particle Reynolds numbers greater than 750, where $\mathrm{Re}_d = uD_P/\nu$, and D_P is the mean particle diameter. Kar and Dybbs [23] proposed

$$\mathrm{Nu}_{sf} = 0.004\,\mathrm{Re}_d^{1.35}\mathrm{Pr}^{1/3} \tag{20}$$

for Re_d smaller than 75. To fill in the range of Re_d, Hwang et al. [5] proposed the use of linear interpolation between Eqs. (19) and (20) to obtain values between $75 < \mathrm{Re}_d < 750$. To use these relations with the proposed model, an equivalent solid sphere particle diameter D_E is introduced, where D_E is the particle diameter that preserves the internal area of the unit cell specified by Eq. (1) for a given porosity and pore diameter. D_E is obtained using the expression for the area to volume ratio for a packed spherical bed [4]

$$D_E = \frac{6(1-\varepsilon)}{\beta} \tag{21}$$

but β is obtained from the unit-cube model (Eq. (3)) for a given porosity and pore diameter. Since the porosity and area-to-volume ratio used in Eq. (21) are for the spherical void geometry, the resulting diameter will not generally correspond to the packed-bed diameter. In fact for a spherical void phase material, the porosities are generally much higher than for packed beds. Figure 12 illustrates the equivalency of the two cases; part (*a*) shows the spherical void geometry and part (*b*) shows the same unit cell with the equivalent solid spherical particle distributed at the eight corners of the cube (this could also be illustrated as a sphere floating in the center of the unit cube). The equivalent particle diameter is used in the Reynolds numbers to obtain estimates of the internal convective heat transfer using the method described above.

Figure 13 shows predictions of the internal convective heat transfer obtained using the above relations combined with the internal area ratio β for the case of water forced through a block of porous foam block heated from one side. The predictions are compared to experimental data reported by Straatman et al. [24] for three foams that are summarized in Table 1. Because the blocks are heated from only one side, the present results are obtained by

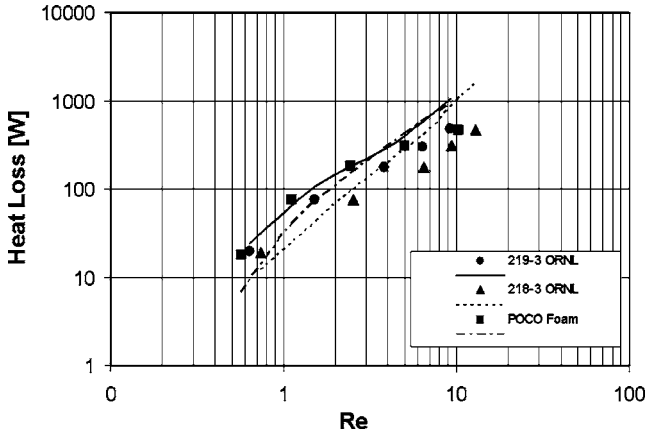

Fig. 13 Plot showing the heat transfer as a function of Re for three porous carbon foam specimens reported by Straatman et al. [24]. The heat transfer is computed using the area-to-volume ratio β combined with the correlations described in Sec. 3.2.

considering the foam block to be an extended surface. In this manner, the area used in the calculation of q is the effective surface area: $A_{\text{eff}}=\eta A_f+A_b$, where η is the equivalent micro-fin efficiency of the foam obtained using the Taylor model [25]; A_f is the interior wall surface area of the foam specimen obtained from $A_f=\beta V$, where V is the volume of the specimen; and A_b is the bare surface area of the heater that is not covered by the porous foam. Figure 13 indicates that the general trends are predicted reasonably well, but that there is some discrepancy, particularly for Re above 5. It is felt that these discrepancies are due mainly to differences in the flow between the spherical void phase foam and the packed spherical bed for which Eq. (20) was devised. Though calibration of the coefficients would lead to better agreement, it is clear that there is a need for research directed at establishing pore-level Nusselt number expressions for spherical void materials that take into account the porosity, pore diameter, and flow characteristics.

4 Hydrodynamic Model

A hydrodynamic model is required to estimate the fluid pressure drop through the inter-connected void structure and thus to estimate the energy necessary to force fluid through the foam. The fluid pressure drop for a porous material is quantified by the Darcy-Forchheimer extended equation [26]

$$\frac{\Delta P}{dx}=\frac{\mu}{K}v+\frac{c_f}{\sqrt{K}}\rho v^2 \tag{22}$$

where v is the filter velocity (based on the open channel flow) at the film temperature, μ is the fluid viscosity, K is the permeability, and c_f is the Forchheimer coefficient (or Ergun's coefficient) determined using the Forchheimer model. Equation (22) is suitable to characterize the pressure drop across a spherical void phase structure provided appropriate values for the permeability and Forchhiemer coefficients are established.

Table 1 Summary of properties for the carbon foam specimens tested by Straatman et al. [24]

Specimen	Porosity (%)	Average Void Dia. (μm)	β[a] (m^2/m^3)	k_{eff} (W/m K)
219-3	86	350	6850	72
218-3	88	400	5640	61
POCO™	82	500	5240	120

[a]As obtained from Eq. (3).

Table 2 Summary of the equivalent particle diameter and *A* and *B* coefficients (see Eqs. (23) and (24)) for the carbon foam specimens tested by Straatman et al. [24]

Specimen	D_E (μm)	A	B
219-3	123	2056	31.8
218-3	128	1841	17.8
POCO™	206	1161	14.9

4.1 Permeability *K*. The most suitable generic expression for the permeability of a packed bed of spheres is given as [14]

$$K=\frac{\varepsilon^3 D_P^2}{A(1-\varepsilon)^2} \tag{23}$$

where D_P is the spherical particle diameter and A is a constant that characterizes the *ease* at which fluid can pass through the porous structure. For a packed bed of spheres, $A=147$ [14]. For a spherical void phase material such as porous carbon foam, the value of A is considerably higher owing to the hydrodynamic pressure loss associated with flow passage through the cell windows connecting the voids. As is evident from Fig. 1, the cell windows can be a wide range of sizes and shapes and differ significantly from the smooth and uniform openings of the unit-cube geometry model. Thus, the unit-cube model represents an ideal structure in terms of the distribution of cell window openings. On the basis of the difference between the predicted and observed cell window openings, it is possible that the unit-cube model slightly underpredicts the internal surface area, however, it is felt the presence of variance and isolated pores more than offsets these differences.

4.2 Forchheimer Coefficient. The Forchhiemer coefficient can be expressed as

$$c_f=\frac{B}{\sqrt{A}\varepsilon^{3/2}} \tag{24}$$

where B is a constant that takes the value 0.65 for a packed bed of spheres. For fibrous materials, B was found to vary between 0.65 and 2.6 [27].

In essence A and B need to be calibrated to give the correct physical balance between the viscous Darcy term and the Forchhiemer form drag term. To use Eq. (22) to predict the pressure drop associated with flow through porous carbon foam, the equivalent particle diameter D_E, obtained using Eq. (21), is used in Eq. (23) and suitable values for A and B are obtained by calibration with the experimental data reported in [24]. As such, the geometry of the foam is characterized in D_E and the fluid resistance is captured by A and B, all of which have been calculated and summarized in Table 2 for the foams described in Ref. [24]. Figure 14 shows the pressure drop as a function of Reynolds number Re for the foams summarized in Tables 1 and 2. The figure clearly shows that the pressure drop for porous carbon foam is well characterized using Eq. (22). For the coefficients used, the trend with Re is reproduced with very high accuracy. The POCO™ foam described in Ref. [24] has a more open internal structure and thus, a much higher permeability and lower pressure drop. In contrast, the 219-3 foam was described as having much poorer interconnectivity between the cells and, thus, a lower permeability and higher pressure drop. This is reflected in the A and B coefficients in Table 2, where both the viscous and form drag terms are noted to be highest for the 219-3 foam.

The unit-cube geometry and the thermal and hydrodynamic models were also used as the basis for a complete thermal engineering model of a water-to-air heat exchanger [28]. The engineering model predicted performance ratings to within 11.5% of

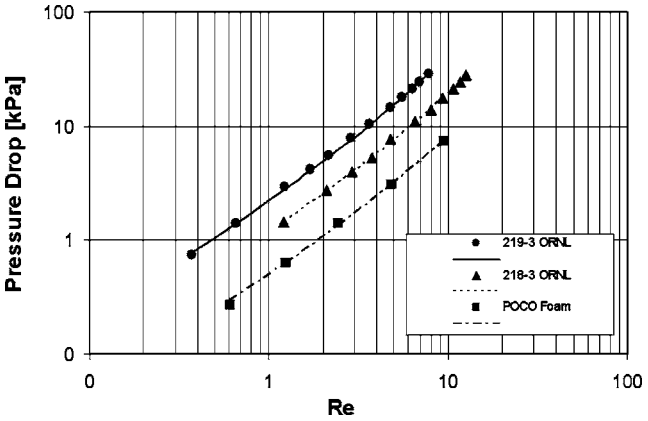

Fig. 14 Plot showing the pressure drop as a function of Re for three porous carbon foam specimens reported by Straatman et al. [24].

those obtained in laboratory experiments, thus further validating the utility of the proposed approach for characterizing porous carbon foam.

5 Summary

An engineering model has been developed for porous carbon foam based on a unit-cube geometry model. The geometry model is based on sphere-centered, interconnected unit cubes, where the spheres represent the fluid or void phase of the porous media. The geometry model was used to derive all of the geometric parameters required to calculate the internal convective heat transfer and pressure drop through the porous material. The model was also used to develop an analytical expression for the effective (stagnant) conductivity of porous carbon foam. The effective conductivity model was developed using a volume equivalency (i.e., by preserving the porosity) and was shown to accurately predict the thermal conductivity as a function of porosity without the need for calibration. Thus, the model has the potential for wide applicability in engineering and CFD models. The internal area ratio β obtained from the unit-cube model was then used in combination with existing expressions for the pore-level Nusselt number to obtain estimates of the heat transfer obtained by passing water through porous carbon foam blocks. Comparisons with experiments showed that while the trends were reasonable, significant discrepancies between the predicted and measured heat transfer were evident at moderate Re, suggesting the need for a Nusselt number expression that is specific to the spherical void phase geometry. In terms of hydrodynamics, comparisons with experimental data showed that the Darcy-Forchhiemer law accurately characterized the pressure drop as a function of Re once the model parameters were properly calibrated. In this regard, further work is also required to express the permeability and Forchhiemer coefficient over a range of porosities and pore diameters.

Acknowledgment

This work was sponsored by the Natural Science and Engineering Research Council of Canada (NSERC) in collaboration with Oak Ridge National Laboratory.

Nomenclature

A = constant
a = square bar of the equivalent square bar structure
B = constant
c_f = Forcheimer coefficient
D = pore (void phase) diameter of the foam
D_E = diameter of the equivalent spherical particle
d_v = equivalent diameter of void phase
h = height of the cube
K = permeability of the foam
k_e = effective thermal conductivity of the foam
k_f = thermal conductivity of the fluid
k_s = thermal conductivity of the solid
Nu = Nusselt number
P = pressure
Pr = Prandtl number
R = radius of the pore, thermal resistance
R_A = absolute surface roughness of the exposed pore surface
R_E = radius of the equivalent spherical particle
Re_d = particle Reynolds number
S = surface area
S_F = surface area factor at the exposed pore surface
v = filter velocity (based on open channel flow)
V = volume

Greek Symbols

β = interior wall surface area to volume ratio
ε = porosity
ε_e = volume ratio of the parallel part to the sum of the series part and the parallel part
ρ = density
μ = viscosity

Subscripts

f = fluid
pb = pore block
s = solid
t = total
v = void

References

[1] Klett, W. J., 2000, "Process for Making Carbon Foam," United State Patent No. 6,033,506.
[2] Klett, W. J., Hardy, R., Romine, E., Walls, C., and Burchell, T., 2000, "High-Thermal Conductivity, Mesophase-Pitch-Derived Carbon Foam: Effect of Precursor on Structure and Properties," Carbon, **38**, pp. 953–973.
[3] Gallego, C. N., and Klett, W. J., 2003, "Carbon Foams for Thermal Management," Carbon, **41**, pp. 1461–1466.
[4] Dullien, F. A. L., 1979, *Porous Media Fluid Transfer and Pore Structure*, Academic, New York.
[5] Hwang, G. J., Wu, C. C., and Chao, C. H., 1995, "Investigation of Non-Darcy Forced Convection in an Asymmetrically Heated Sintered Porous Channel," ASME J. Heat Transfer, **117**, pp. 725–731.
[6] Paek, W. J., Kang, H. B., Kim, Y. S., and Hyum, M. J., 2000, "Effective Thermal Conductivity and Permeability of Aluminum Foam Materials," Int. J. Thermophys., **21**(2), 453–464.
[7] Deissler, R. G., and Boegli, J. S., 1958, "An Investigation on Effective Thermal Conductivity of Powders in Various Gases," Trans. ASME, October, pp. 1417–1425.
[8] Batchelor, G. K., and O'Brien, R. W., 1977, "Thermal or Electrical Conduction Through a Granular Material," Proc. R. Soc. London, Ser. A, **355**, pp. 313–333.
[9] Luikov, A. V., Shashkov, A. G., Vasiliev, L. L., and Fraiman, Y. E., 1968, "Thermal Conductivity of Porous System," Int. J. Heat Mass Transfer, **11**, pp. 117–140.
[10] Bhattacharya, A., Calmidi, V. V., and Mahajan, R. L., 2002, "Thermophysical Properties of High Porosity Metal Foams," Int. J. Heat Mass Transfer, **45**, pp. 1017–1031.
[11] Tee, C. C., Klett, J. W., Stinton, D. P., and Yu, N., 1999, "Thermal Conductivity of Porous Carbon fFam," *Proceedings of the 24th Biennial Conference on Carbon*, Charleston, SC.
[12] Klett, J. W., McMillan, A. D., Gallego, N. C., and Walls, C., 2004, "The Role of Structure on the Thermal Properties of Graphitic Foams," J. Mater. Sci., **39**, 3659–3676.
[13] Ergun, S., 1952, "Fluid Flow Through Packed Columns," Chem. Eng. Prog., **48**, pp. 89–94.
[14] Nakayama, A., and Kuwahara, F., 2000, "Numerical Modeling of Convective Heat Transfer in Porous Media Using Microscopic Structures," in *Handbook of Porous Media*, K. Vafai and H. A. Hadim, eds., Marcel Dekker, New York, 449 pp.
[15] Ward, C. J., 1964, "Turbulent Flow in Porous Media," J. Hydraulics Division, Proceeding of the American Society of the Civil Engineers, HY5, pp. 1–11.

[16] Kaviany, M., 1995, *Principles of Heat Transfer in Porous Media*, 2nd ed., Springer, New York.
[17] Bear, J., and Corapcioglu, M. Y., 1984, *Fundamentals of Transport Phenomena in Porous Media*, J. Bear and M. Y. Corapcioglu, eds., Martinus Nijhoff, Dordrecht.
[18] Bear, J., and Corapcioglu, M. Y., 1987, *Advances in Transport Phenomena in Porous Media*, J. Bear and M. Y. Corapcioglu, eds., Martinus Nijhoff, Dordrecht.
[19] Bear, J., and Corapcioglu, M. Y., 1991, *Transport Processes in Porous Media*, J. Bear and M. Y. Corapcioglu, eds., Kluwer Academic, Dordrecht.
[20] Kakac, S., Killis, B., Kulacki, A. F., and Arinc, F., 1991, *Convetinve Heat and Mass Transfer in Porous Media*, S. Kakac, B. Killis, F. A. Kulacki, and F. Arinc, eds., Kluwer Academic, Dordrecht.
[21] Vafai, K., and Hadim, A. H., 2000, *Handbook of Porous Media*, K. Vafai and H. A. Hadim, eds., Marcel Dekker, New York.
[22] Gamson, B. W., Thodos, G., and Hougen, O. A., 1943, "Heat, Mass and Momentum Transfer in the Flow Gases Through Granular Solid," Trans. Am. Inst. Chem. Eng., **39**, pp. 1–35.
[23] Kar, K. K., and Dybbs, A., 1982, "Internal Heat Transfer Coefficients of Porous Metals," in *Heat Transfer in Porous Media*, J. V. Beck and L. S. Yao, eds., HTD-22, ASME.
[24] Straatman, A. G., Gallego, N. C., Yu, Q., and Thompson, B. E., 2005, "Characterization of Porous Carbon Foam as a Material for Compact Recuperators," *Proceedings of ASME Turbo Expo 2006*, Paper No. GT2006–50958, Barcelona, Spain, May 2006.
[25] Taylor, G. I., 1971, "A Model for the Boundary Condition of a Porous Material. Part 1," J. Fluid Mech., **49**, pp. 319–326.
[26] Dybbs, A., and Edwards, R. V., 1984, "A New Look at Porous Media Fluid Mechanics-Darcy to Turbulent," in *Fundamentals of Transport Phenomena in Porous Media*, J. Bear and M. Y. Corapcioglu, eds., Martinus Nijhoff, Dordrecht, pp. 199–254.
[27] Tadrist, L., Miscevic, M., Rahli, O., and Topin, F., 2004, "About the Use of Fibrous Materials in Compact Heat Exchangers," Exp. Therm. Fluid Sci., **28**, pp. 193–199.
[28] Yu, Q., Straatman, A. G., and Thompson, B. E., 2006, "Carbon Foam Finned-Tubes in Air-Water Heat Exchangers," Appl. Therm. Eng., **26**, pp. 131–143.